Available online at www.sciencedirect.com
SCIENCE DIRECT®
International Journal of Solids and Structures 43 (2006) 5337–5354
INTERNATIONAL JOURNAL OF SOLIDS and STRUCTURES
www.elsevier.com/locate/ijsolstr

Material cloud method—its mathematical investigation and numerical application for 3D engineering design

Su-Young Chang [a], Sung-Kie Youn [b,*]

[a] *Computational Engineering Science Laboratory, Department of Mechanical Engineering, Korea Advanced Institute of Science and Technology, 373-1, Guseong-dong, Yuseong-gu, Daejeon 305-701, Republic of Korea*
[b] *Department of Mechanical Engineering, Korea Advanced Institute of Science and Technology, 373-1, Guseong-dong, Yuseong-gu, Daejeon 305-701, Republic of Korea*

Received 22 April 2005
Available online 5 October 2005

Abstract

Recently, material cloud method (MCM) has been developed as a new approach for topology optimization. In MCM, an optimal structure can be obtained by manipulating the sizes and positions of material clouds, which are material patches with finite sizes and constant material densities, and the numerical analysis can be done using fixed background finite element mesh. During the optimization procedure, only active elements, where more than one material cloud is contained, are treated. With MCM, an expansion–reduction procedure of the design domain can be naturally realized through movements of material clouds, so that a true optimal solution can be found without any significant increase of computational costs. In this paper, we summarize the concept of MCM and prove the existence of optimal solution(s) in the formulation of MCM to show the mathematical rigorousness of this new method. We show the design examples for 3D engineering design problems to show the generality of this method.

Keywords: Topology optimization; Material cloud method (MCM); Design domain; Existence-proof; 3D engineering design

1. Introduction

Since Bendsoe and Kikuchi's (1988) pioneering work, topology optimization method has become popular and has been successfully applied into industrial design (Sigmund, 2001; Chang et al., 2001; Park et al.,

* Corresponding author. Tel.: +82 42 869 3034; fax: +82 42 869 3210.
E-mail address: skyoun@sorak.kaist.ac.kr (S.-K. Youn).

0020-7683/$ - see front matter © 2005 Elsevier Ltd. All rights reserved.
doi:10.1016/j.ijsolstr.2005.07.039

2003). Bendsoe and Sigmund (2003) have systematically investigated the theory, methods and applications of topology optimization.

Though the traditional density-based approach (Bendsoe, 1989; Yang and Chuang, 1994) has been most commonly used for topology optimization due to its simplicity and good harmony with FEM, this approach has some complications like checkerboard-pattern and mesh-dependency that significantly influence the computational results (Bendsoe and Sigmund, 2003).

Also another important complication to note is that the density-based approach can yield optimal solution for a given design space (Kim and Kwak, 2002). Therefore, the obtained optimal result depends on the size and shape of the design space. In this sense, the obtained topology may not be the truly optimized one.

Recently, various new topology optimization techniques have been emerging in order to circumvent some difficulties encountered in applications of the traditional density approach or density distribution method (DDM).

First one is a level set approach (Sethian and Wiegmann, 2000; Belytschko et al., 2003). In this approach, a level set function or implicit function is introduced to identify the material domain and the occurrence of checkerboard-pattern can be avoided.

Second one is an element connectivity parameterization (ECP) approach (Yoon and Kim, 2005). In this approach, all finite elements are kept solid throughout the optimization process and zero-length elastic links are introduced to parameterize inter-element connectivity. A reasonable optimal solution can be obtained for the geometrically nonlinear topology optimization problems.

Third one is various researches for an expansion and reduction of design domain or design space during topology optimization procedure (Xie and Steven, 1993; Querin et al., 1998; Kim et al., 2003; Liu et al., 2000; Kim and Kwak, 2002; Chang et al., 2004; Chang and Youn, in press). In the traditional density-based approach (DDM), design domain is fixed as initially defined one and all elements in design domain should be treated and other domain out of the initial design domain cannot be additionally treated irrespective of the values of design variables throughout the optimization procedure. If the design domain or design space can be adaptively modified depending on some information during design procedure, a better optimal design can be obtained with reduced computational costs.

Xie and Steven (1993), Querin et al. (1998), and Kim et al. (2003) proposed an evolutionary structural optimization (ESO) approach, in which design space is element-wise reduced or expanded. Liu et al. (2000) proposed a metamorphic development (MD) method, in which the optimization proceeds by metamorphic development of a structure. Kim and Kwak (2002) proposed a design space optimization technique, in which the design space is concurrently optimized with the design variables in the traditional density-based approach.

In the aforementioned researches to modify the design domain or design space, the criteria to decide whether a certain element should be added or excluded are arbitrary, depending on the application problem. On the other hand, pretty high computational costs are additionally required to calculate the information related with the criteria.

Chang et al. (2004) and Chang and Youn (in press) proposed a new topology optimization approach named material cloud method (MCM) and showed the results of MCM, compared with those of the traditional density-based approach for several 2D linear static design problems. In MCM, the modification of design domain can be naturally and efficiently accomplished only depending on the change of values of design variables. In MCM, the design variables are central positions and sizes of material clouds, which are independent material patches. The basic idea of MCM is to free the material from the computational mesh, so that the material patches can be moved freely and independently with one another. By doing so, we can resolve two significant obstacles in the traditional density-based method. First of all, if we provide enough space for the material patches to move around, we can find a truly optimized topology without having to rely on any special schemes for design-space modification. In doing so, we only need to track the material patches and only the elements, which contain certain portion of any material patches, will be involved in the

computation. Therefore, unlike in the traditional DDM, where every single element in the design space needs to be treated in the computation, one can significantly reduce the number of elements involved during the optimization process.

Cheng and Olhoff (1981) has pointed out the nonexistence of optimal solution(s) for an optimal thickness problem of plates by some numerical experiments. Since then, Bendsoe (1984) indicated that the reason for this nonexistence is the nonclosedness of the set of deflection functions corresponding to the set of admissible designs and showed that existence could be obtained if a bound on the gradient of the thickness function was imposed. A consequence of this nonexistence is that even if each discretization of the unrestricted problem is well posed, these solutions do not converge to a macroscopic design when the discretization parameter tends to 0, and thinner patterns are exhibited. This phenomenon is often also referred to in the literature as mesh dependency (Bourdin, 2001). To guarantee the existence of solutions, various kinds of methods have been introduced (Bendsoe and Sigmund, 2003). One is a homogenization method, in which the set of admissible domains is enlarged including the microstructures (Bendsoe and Kikuchi, 1988). Another approach is to add additional constraints on the set of admissible designs like an upper bound on the perimeter of the resulting design (Ambrosio and Buttazzo, 1993; Beckers, 1999) or an upper bound on the gradients of density function (Petersson and Sigmund, 1998). The third is a filtering method for a density function (Bourdin, 2001) or a sensitivity (Sigmund, 1997).

In this paper, we prove the existence of optimal solution(s) in MCM to show the mathematic rigorousness of this method and extend the application of MCM into 3D engineering design to show the generality of this method.

The outline of this paper is as follows. In Section 2, basic concept and numerical formulation of MCM are summarized. In Section 3, the existence of optimal solutions(s) is proved. In Section 4, the optimal results for 3D engineering problem are shown, compared with those of the traditional density-based method. Finally, concluding remarks are given in Section 5.

2. Overview of the material cloud method (MCM)

In this section, we will shortly explain the basic optimization concept and numerical procedure of MCM, which was prescribed in the previous research of MCM (Chang et al., 2004; Chang and Youn, in press). For the sake of convenience, the compliance minimization problem for a 2D linear elastic structure will be treated.

In MCM, an optimal design is to be extracted from the distribution of material clouds and the design variables are the central positions and sizes of material clouds. The material cloud is a finite material patch with a constant relative density of material as in Fig. 1. It is assumed that the shape of a material cloud is a square for 2D problem or a cube for 3D problem.

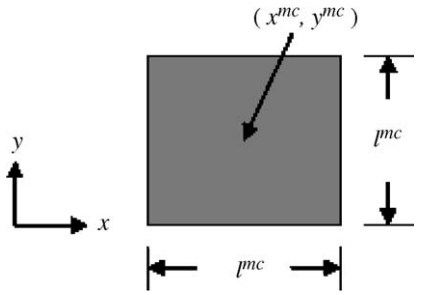

Fig. 1. Material cloud (for 2D problem).

In this research, there are three different ways of applying MCM for topology optimization. One is to optimize only central positions of material clouds, named MCMP. Another is to optimize only sizes of material clouds, named MCMS. The third is to optimize central positions of material clouds and subsequently to optimize sizes of material clouds, named MCMPS.

2.1. MCMP

Firstly, the optimization concept of MCMP will be explained.

In MCMP, material clouds can move around independently crossing the element-boundary and overlap one another under one condition that the sum of equivalent areas of material clouds contained in each element should not exceed the area of the element, which is an upper bound in physical sense.

An active element is defined as an element in which more than one material cloud is contained and an active node is defined as a node which constitutes the active element and an active DOF is defined as a DOF related to the active node.

Fig. 2 depicts the optimization procedure of MCMP.

The procedure of MCMP is as follows:

(1) Step 1: Define a design domain and a sub-domain where material clouds are initially distributed (Fig. 2(a)).
(2) Step 2: Allocate material clouds in all elements of the sub-domain (Fig. 2(a)).
(3) Step 3: Modify positions of material clouds until a convergence condition is satisfied (Fig. 2(b)–(d)).
(4) Step 4: Extract an optimal design form a converged distribution of material clouds (Fig. 2(e)).

In Fig. 2(a), the sub-domain is defined as a part of the whole design domain. In this case, the expansion of the sub-domain can be naturally realized through the movements of material clouds. Utilizing this expansion procedure, a true optimal design on a larger design domain can be obtained without any significant increase of computational costs.

At the initial optimization step, one material cloud per element on the sub-domain is allocated at the center of the element. An area of material cloud, A_i^{mc} is specified by user, which should be not smaller than the size of an element, and then relative density of material cloud, ρ_i^{mc} is determined by Eq. (1), which means the ratio of a density of material cloud to a density of real material used in design. In Eq. (1), $\widehat{A}_i^{\mathrm{mc}}$ is an equivalent area of material cloud and A_i^{elem} is an area of element, where the material cloud is allocated. A constant, $\alpha\ (\in(0,1))$ is initially given considering the allowable total amount of material in design. If the computational mesh is uniform, all material clouds have same equivalent area:

$$\widehat{A}_i^{\mathrm{mc}} = \rho_i^{\mathrm{mc}} \times A_i^{\mathrm{mc}}\left(\text{or } (l_i^{\mathrm{mc}})^2\right) = \alpha \times A_i^{\mathrm{elem}}. \tag{1}$$

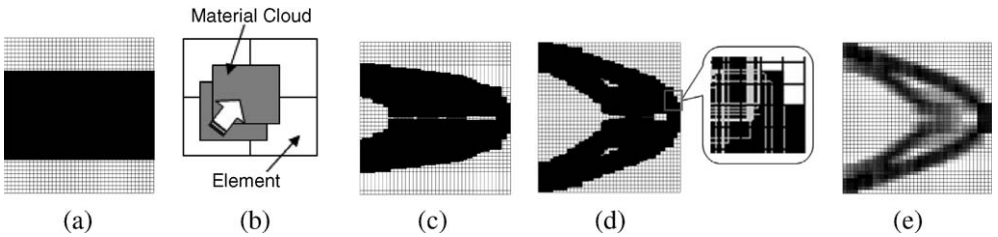

Fig. 2. Optimization procedure of MCMP: (a) initial distribution of material clouds, (b) modification of positions of material clouds, (c) distribution of material clouds during iterations, (d) converged distribution of material clouds, and (e) distribution of equivalent densities of elements corresponding to (d).

In Fig. 2(d), the enlarged view of the distribution of material clouds can be seen on a certain part of design domain. It is observed that material clouds are overlapped one another. Fig. 2(e) shows a distribution of equivalent densities of active elements corresponding to the result of Step 3, which will be used as a criterion for extraction of an optimal design. The equivalent density of an active element is determined by the amount of material clouds contained in that element, which will be quantitatively defined later in this section. However, due to the finite sizes and number of material clouds, the topology obtained by MCMP is not clear.

Next detailed numerical procedure of MCMP will be described.

The optimization problem can be stated like

$$\begin{aligned} &\text{Minimize} && f(\boldsymbol{b}) \\ &\text{subject to} && g(\boldsymbol{b}) \leqslant 0, \\ & && \boldsymbol{b}_{\text{lb}} \leqslant \boldsymbol{b} \leqslant \boldsymbol{b}_{\text{ub}}, \end{aligned} \tag{2}$$

where $\boldsymbol{b} = [b_1 \;\; b_2 \;\; \cdots \;\; b_{N_{\text{dv}}-1} \;\; b_{N_{\text{dv}}}]^{\text{T}}$, N_{dv}: number of design variables.

In MCMP, design variables, $\boldsymbol{b}$ are the central positions of square-shape material clouds, $(x_i^{\text{mc}}, y_i^{\text{mc}})$. The number of design variables, N_{dv} is twice the number of material clouds, N_{mc} in 2D problem. The number of material clouds, N_{mc} equals to the number of elements in the initial sub-domain. The area of an ith material cloud, A_i^{mc} and the relative density of the material cloud, ρ_i^{mc} are fixed throughout the optimization procedure.

The objective function, which is the compliance for a linear static problem, is defined by

$$f(\boldsymbol{b}) = \int_{\Omega^{\text{ADD}}(\boldsymbol{b})} \boldsymbol{r}(\boldsymbol{b}) \cdot \boldsymbol{u}(\boldsymbol{b}) \, \mathrm{d}\Omega + \int_{\Gamma_t} \boldsymbol{t} \cdot \boldsymbol{u}(\boldsymbol{b}) \, \mathrm{d}s. \tag{3}$$

In Eq. (3), the active design domain, Ω^{ADD} is a domain which consists of all active elements and may be changed during the optimization process. It is assumed that the traction surface, Γ_t and the traction, $\boldsymbol{t}$ are independent on the design. And $\boldsymbol{r}$ and $\boldsymbol{u}$ are a body force and a displacement, respectively.

Before calculating the state-variable like the displacement of a structure, the density of an element for all active elements should be defined. The density of an element, ρ_j^{elem} is a ratio of a sum of equivalent areas of material clouds contained in the element to the size of the element. In MCMP, this value can be defined as in Eq. (4). It can be easily calculated in the case of rectangular regular meshes and square material clouds as follows:

$$\rho_j^{\text{elem}} = \frac{\sum_{i=1}^{N_{\text{mc}}} \left[(A_j^{\text{elem}} \cap A_i^{\text{mc}}) \times \rho_i^{\text{mc}} \right]}{A_j^{\text{elem}}}. \tag{4}$$

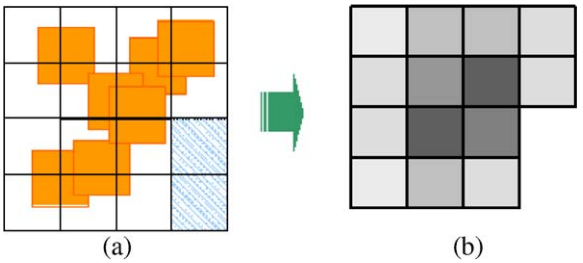

Fig. 3. Distribution of the density of an element corresponding to an arbitrary distribution of material clouds: (a) arbitrary distribution of material clouds and (b) distribution of the density in active elements.

Fig. 3 illustrates the concept of the density of an element in MCMP. In Fig. 3(a), two shaded elements are not active elements. Fig. 3(b) shows the corresponding distribution of the density of an element for the particular distribution of material clouds of Fig. 3(a).

The displacement field of a structure can be solved by

$$\left.\begin{aligned} &\boldsymbol{K}\cdot\boldsymbol{U}=\boldsymbol{F}\\ &\text{where } \boldsymbol{K}=\sum_{j=1}^{N_{\text{elem}}}\boldsymbol{k}_j,\\ &\qquad \boldsymbol{F}=\sum_{j=1}^{N_{\text{elem}}}\boldsymbol{f}_j,\\ &\qquad \boldsymbol{k}_j=\rho_j^{\text{elem}}\int_{\Omega_j}\boldsymbol{B}_j^{\mathrm{T}}\cdot\boldsymbol{D}_j\cdot\boldsymbol{B}_j\,\mathrm{d}\Omega,\\ &\qquad \boldsymbol{f}_j=\int_{\Omega_j}\boldsymbol{N}\cdot\boldsymbol{r}(\rho_j^{\text{elem}})\,\mathrm{d}\Omega+\int_{\partial\Omega_j}\boldsymbol{N}\cdot\boldsymbol{t}\,\mathrm{d}s. \end{aligned}\right\} \tag{5}$$

In Eq. (5), N_{elem} means the number of active elements and Ω_j is the domain of an jth element and element-stiffness matrix, $\boldsymbol{k}_j$ is proportional to the density of the element without a penalization of an intermediate density, which is a physical upper bound (Swan and Kosaka, 1997).

The sensitivity of the objective function can be easily calculated as in the case of the traditional density approach. The reason why the size of a material cloud should not be smaller than the size of an element is that the continuous sensitivity of the objective function should be obtained irrespective of the position of a material cloud. If a material cloud which is smaller than the size of an element is completely included in a certain element, the sensitivity of the objective function may be vanished. In this case, this material cloud cannot change its position throughout the optimization process.

Side constraints of design variables in Eq. (2) can be determined considering following three simple conditions. The first is that material clouds should be contained in the design domain. The second is that a density of element in all active elements should be less than one, which is the physical limit. The third is a move-limit, which is usually set up as the half of the size of an element.

Since all material clouds are coercively maintained in design domain by the side constraint, the inequality constraint on the amount of material in design needs not to be considered.

Instead, an inequality constraint on the sum of movements of material clouds as in Eq. (6) is considered to achieve a consistent convergence of design variables during optimization process. In Eq. (6), the constant, C_g is the sum of allowable movements of material clouds determined by side constraints and the constant, $\alpha\in(0,1)$ is usually set up as 0.5 in this research. In Eq. (6), $(x_i^{\text{mc}})_p$ and $(y_i^{\text{mc}})_p$ are the x- and y-coordinates of the ith material cloud at the previous iteration, respectively:

$$g(\boldsymbol{b})=\sum_{i=1}^{N_{\text{mc}}}\left(\left|x_i^{\text{mc}}-(x_i^{\text{mc}})_p\right|+\left|y_i^{\text{mc}}-(y_i^{\text{mc}})_p\right|\right)-\alpha\times C_g\leqslant 0. \tag{6}$$

The sensitivity of the inequality constraint can be uniquely determined through restricting admissible ranges of design variables considering the sensitivity of the objective function, as

$$\frac{\partial g}{\partial b_i}=\begin{cases} 1, & \text{if } \dfrac{\partial f}{\partial b_i}<0,\\ 0, & \text{if } \dfrac{\partial f}{\partial b_i}=0,\\ -1, & \text{if } \dfrac{\partial f}{\partial b_i}>0. \end{cases} \tag{7}$$

In MCMP, an optimization algorithm based on the optimality criteria method developed by Diaz and Kikuchi (1992) and Ma et al. (1995) is used. This algorithm was originally developed for topology

optimization of an eigenvalue problem, but has been successfully applied into various kinds of problems including static problems (Chang et al., 2001; Park et al., 2003). In this algorithm, only one inequality constraint can be treated. If additional constraints should be considered, MMA algorithm (Svanberg, 1987, 2002), in which more constraints can be treated, could be employed.

2.2. MCMS

Firstly, the optimization concept of MCMS will be explained.

In MCMS, a material cloud can grow and shrink only in the element where it is initially allocated, but cannot be vanished. Therefore, material clouds cannot be overlapped each other and the active design domain, which consists of all active elements, cannot be changed from initially defined whole design domain. Relative densities of material clouds are specified as unity and then initial areas of material clouds are determined similarly to the case of MCMP by Eq. (1).

Fig. 4 depicts the optimization procedure of MCMS.

The procedure of MCMS is as follows:

(1) Step 1: Define a design domain (Fig. 4(a)).
(2) Step 2: Allocate material clouds in all elements of the design domain (Fig. 4(a)).
(3) Step 3: Modify sizes of material clouds until a convergence condition is satisfied (Fig. 4(b)–(d)).
(4) Step 4: Extract an optimal design from a converged distribution of material clouds (Fig. 4(d)).

At Step 2, one material cloud is allocated in each element and the central position of the material cloud is identical to the center of the element. In Fig. 4(c), sizes of material clouds are varied in a range from a very small value to the size of an element. By MCMS, a clear optimal design configuration is obtained as shown in Fig. 4(d).

Next detailed numerical procedure of MCMS will be described.

In MCMS, design variables, $\boldsymbol{b}$ are the sizes of square-shape material clouds. The number of design variables, N_{dv} is the number of material clouds, N_{mc}. The number of material clouds, N_{mc} equals to the number of elements in the design domain. The size of a material cloud may be represented by the area, A_i^{mc} or the length, l_i^{mc} of a material cloud. The central position of a material cloud, $(x_i^{\mathrm{mc}}, y_i^{\mathrm{mc}})$ and the relative density of a material cloud, ρ_i^{mc} are fixed throughout the optimization process.

The objective function, which is the compliance for a linear static problem, is defined as

$$f(\boldsymbol{b}) = \int_{\Omega^{\mathrm{MCD}}(\boldsymbol{b})} \boldsymbol{r}\cdot\boldsymbol{u}(\boldsymbol{b})\,\mathrm{d}\Omega + \int_{\Gamma_t} \boldsymbol{t}\cdot\boldsymbol{u}(\boldsymbol{b})\,\mathrm{d}s. \tag{8}$$

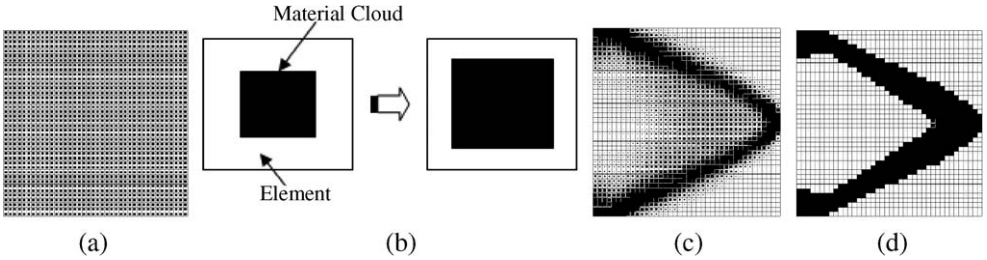

Fig. 4. Optimization procedure of MCMS: (a) initial distribution of material clouds, (b) modification of sizes of material clouds, (c) distribution of material clouds during iterations, (d) converged distribution of material clouds.

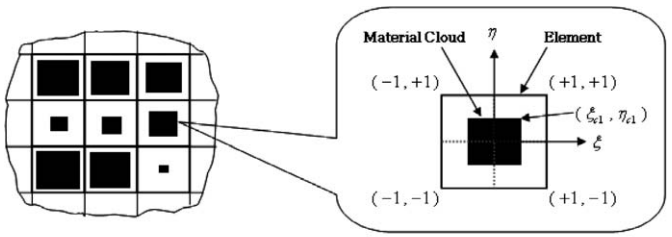

Fig. 5. Material cloud domain and integration domain in MCMS: (a) material cloud domain and (b) integration domain for one material cloud.

In Eq. (8), Ω^{MCD} is the material cloud domain, which is the domain occupied by all material clouds (black region in Fig. 5(a)). It is assumed that the traction surface, Γ_t, the traction, $\boldsymbol{t}$ and the body force, $\boldsymbol{r}$ are independent on the design.

In this section, all descriptions will be made for the case when the area of a material cloud, A_i^{mc} is used as a design variable.

In MCMS, the density of an element, ρ_j^{elem} can be defined as follows:

$$\rho_j^{\mathrm{elem}} = \frac{A_j^{\mathrm{mc}}}{A_j^{\mathrm{elem}}}. \tag{9}$$

The displacement field of a structure can be solved by

$$\left.\begin{aligned} &\boldsymbol{K}\cdot\boldsymbol{U} = \boldsymbol{F},\\ &\text{where } \boldsymbol{K} = \sum_{j=1}^{N_{\mathrm{elem}}} \boldsymbol{k}_j,\\ &\qquad \boldsymbol{F} = \sum_{j=1}^{N_{\mathrm{elem}}} \boldsymbol{f}_j,\\ &\qquad \boldsymbol{k}_j = P(\rho_j^{\mathrm{elem}}) \int_{\Omega_j^{\mathrm{mc}}} \boldsymbol{B}_j^{\mathrm{T}}\cdot\boldsymbol{D}_j\cdot\boldsymbol{B}_j \,\mathrm{d}\Omega,\\ &\qquad \boldsymbol{f}_j = \int_{\Omega_j^{\mathrm{mc}}} \boldsymbol{N}\cdot\boldsymbol{r}\,\mathrm{d}\Omega + \int_{\partial\Omega_j} \boldsymbol{N}\cdot\boldsymbol{t}\,\mathrm{d}s. \end{aligned}\right\} \tag{10}$$

For the calculation of the element-stiffness matrix, $\boldsymbol{k}_j$ in Eq. (10), the integration domain is the domain of the material cloud contained in the element, Ω_j^{mc} (Fig. 5(b)). The element-stiffness matrix, $\boldsymbol{k}_j$ is penalized by a material property function, $P(\rho_j^{\mathrm{elem}})$, so that the densities of elements are converged to unity or to a very small value as in the traditional density approach. In this research, an exponential function is used as the penalization function of the material property. As previously described, the integration domain is shrunk in proportion to the ratio of the area of the material cloud, Ω_j^{mc} to the area of the corresponding element, Ω_j. Thus compared with the case of the traditional density approach, one-order lower exponent, $n = 2$ is used in order to apply a similar effect of penalization.

One inequality constraint on the allowable amount of material is considered. In Eq. (11), A_0 is an allowable maximum area of material:

$$g(\boldsymbol{b}) = \int_{\Omega^{\mathrm{MCD}}} \mathrm{d}\Omega - A_0 = \sum_{i=1}^{N_{\mathrm{mc}}} [A_i^{\mathrm{mc}}] - A_0 \leqslant 0. \tag{11}$$

In Eq. (2), the upper bound and the lower bound of design variables are the size of an element and very small value, respectively.

The sensitivity of the objective function and the inequality constraint can be easily calculated numerically as in the case of the traditional density approach.

As an optimization algorithm, the optimality criteria-based algorithm in the case of MCMP is identically used.

In MCMS, lower-order elements or higher-order elements may be used. The checkerboard-pattern in the case of lower-order elements can be suppressed with a density redistribution algorithm used in the traditional density approach (Youn and Park, 1997; Swan and Kosaka, 1997). In this research, we used higher-order elements without any special scheme (Jog and Haber, 1996).

The optimization procedure of MCMS may seem to be similar with that of the traditional density approach like SIMP (solid isotropic material with penalization; Bendsoe and Sigmund, 2003). But due to the difference of optimization concepts, even though the same optimization algorithm is applied, the convergence and final results are quite different from those of SIMP. This fact can be obviously observed in the numerical examples of Chang et al. (2004) and Chang and Youn (in press).

2.3. MCMPS

In MCMPS, MCMP and MCMS are sequentially applied.

Fig. 6 depicts the optimization procedure of MCMPS.

The application procedure of MCMPS is as follows:

(1) Step 1: Define a design domain and a sub-domain where material is initially distributed (Fig. 6(a)).
(2) Step 2: Allocate material clouds in all elements of the sub-domain (Fig. 6(a)).
(3) Step 3: Modify positions of material clouds by MCMP until a convergence condition is satisfied (Fig. 6(b)).
(4) Step 4: From the result of Step 3, determine the equivalent sizes of material clouds in all active elements (Fig. 6(c)–(d)).
(5) Step 5: Modify sizes of material clouds by MCMS until a convergence condition is satisfied (Fig. 6(e)).
(6) Step 6: Extract an optimal design from the converged distribution of material clouds (Fig. 6(e)).

Except Step 4, all other procedures are identical to those of MCMP and MCMS. The result of material distribution after MCMP is used as the initial distribution for the subsequent MCMS (Fig. 6(b)–(d)). At the initial distribution for MCMS, the size of a material cloud can be determined by Eq. (12). In Eq. (12), ρ_i^{elem} is the density of an element when MCMP is terminated (Fig. 6(c)). Fig. 6(d) shows a re-initialized distribution of material clouds for the subsequent MCMS. By MCMPS, a clear optimal distribution is obtained as shown in Fig. 6(e):

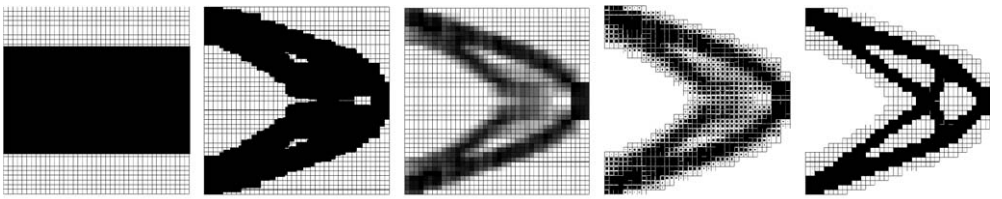

Fig. 6. Optimization procedure of MCMPS: (a) initial distribution of material clouds for MCMP, (b) converged distribution of material clouds after MCMP, (c) distribution of equivalent densities of elements corresponding to (b), (d) initial distribution of material clouds for subsequent MCMS, and (e) final material distribution after MCMS.

$$A_i^{\mathrm{mc}} = A_i^{\mathrm{elem}} \times \rho_i^{\mathrm{elem}}. \tag{12}$$

In MCMPS, the design domain can be naturally expanded and reduced through movements of material clouds by MCMP and a clear resulting topology can be obtained with fast convergence by subsequent MCMS (Chang and Youn, in press).

3. Proof of existence of optimal solutions

In this paper, we show the existence of optimal solution(s) for a case of MCMP where finite material clouds are used with a corresponding computational mesh. In MCMS, the (active) design domain is fixed throughout the optimization procedure, so the existence-proof can be trivially shown, following the mathematical analysis by Petersson and Sigmund (1998). Moreover, it can be said that this for MCMPS is shown considering both results of MCMP and MCMS.

The procedure of existence-proof by Petersson and Sigmund (1998) is much referred in this research. Petersson and Sigmund (1998) proved that finite elements solutions corresponding to different mesh sizes converged the exact solution(s) for slope-constrained density-based topology optimization problem.

The existence-proof procedure in MCMP is not trivial like the case of the density-based approach for a finite computational mesh, because the active design domain in MCMP is changed throughout the optimization procedure. Until now, there is no research about the mathematical analysis for this kind of optimization problem, where the design domain or design space may be changed during optimization procedure.

3.1. The existence-proof in MCMP

In this section, we treat the optimization procedure of MCMP where the compliance is to be minimized for 2D linear elastic structure. The procedure and result of this section can be easily extended also for 3D problem.

For the convenience of following the mathematical procedure, refer Fig. 7, which define a typical compliance minimization problem. In Fig. 7, Ω is a whole design domain for MCMP.

The discretized minimum compliance problem, $(\mathrm{MC})_h$ corresponding to a computational mesh with mesh size, h is defined as in Eq. (13). We follow the notation used by Petersson and Sigmund (1998). In Eq. (13), Ω^{ADD} is the active design domain and is marked as gray-region in Fig. 8 for a certain design. The function, $l_{\boldsymbol{b}_h}(\cdot)$ and the function, $a_{\boldsymbol{b}_h}(\cdot,\cdot)$ are the compliance (or external work) and the internal energy corresponding to a design, $\boldsymbol{b}_h$, respectively:

$$(\mathrm{MC})_h \begin{cases} \text{Find } (\boldsymbol{u}_h^*, \boldsymbol{b}_h^*) \in V_h|_{\Omega^{\mathrm{ADD}}(\boldsymbol{b}_h^*)} \times H_h \\ \text{such that } \quad a_{\boldsymbol{b}_h^*}(\boldsymbol{u}_h^*, \boldsymbol{v}_h) = l_{\boldsymbol{b}_h^*}(\boldsymbol{v}_h), \ \ \forall \boldsymbol{v}_h \in V_h|_{\Omega^{\mathrm{ADD}}(\boldsymbol{b}_h^*)}, \quad \text{and} \quad l_{\boldsymbol{b}_h^*}(\boldsymbol{u}_h^*) \leqslant l_{\boldsymbol{b}_h}(\boldsymbol{u}_h) \\ \text{for all } (\boldsymbol{u}_h, \boldsymbol{b}_h) \in V_h|_{\Omega^{\mathrm{ADD}}(\boldsymbol{b}_h)} \times H_h \quad \text{satisfying } a_{\boldsymbol{b}_h}(\boldsymbol{u}_h, \boldsymbol{v}_h) = l_{\boldsymbol{b}_h}(\boldsymbol{v}_h), \ \ \forall \boldsymbol{v}_h \in V_h|_{\Omega^{\mathrm{ADD}}(\boldsymbol{b}_h)}. \end{cases} \tag{13}$$

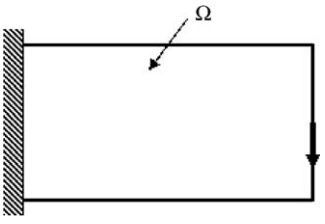

Fig. 7. Definition of a typical optimization problem in MCMP.

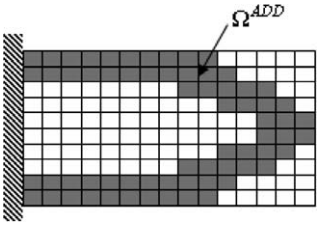

Fig. 8. An active design domain.

In Eq. (13), H_h is a set of admissible designs for the discretized optimization problem, defined in Eq. (14). In Eq. (14), N is the number of material clouds. The set, H_h is a bounded and closed finite dimensional space, so that it is compact by Heine–Borel Theorem (Oden and Demkowicz, 1996):

$$H_h = \left\{ \boldsymbol{b}_h = (\boldsymbol{x}^{\mathrm{T}}, \boldsymbol{y}^{\mathrm{T}})^{\mathrm{T}} \subset R^N \times R^N \mid g(\boldsymbol{b}_h) \leqslant 0,\ \boldsymbol{x}_{\mathrm{lb}} \leqslant \boldsymbol{x} \leqslant \boldsymbol{x}_{\mathrm{ub}},\ \boldsymbol{y}_{\mathrm{lb}} \leqslant \boldsymbol{y} \leqslant \boldsymbol{y}_{\mathrm{ub}},\ \text{Ellipticity condition holds} \right\}. \tag{14}$$

In Eq. (13), $V_h|_{\Omega^{\mathrm{ADD}}(\boldsymbol{b}_h)}$ is a set of kinematically admissible displacements corresponding to a design, $\boldsymbol{b}_h$, as defined in Eq. (15). And $V_h|_{\Omega}$ is a set of kinematically admissible displacements defined on the whole design domain, Ω, as defined in Eq. (16). N_{ae} is the number of active elements for a design, $\boldsymbol{b}_h$ and N_e is the number of total elements in Ω. P_l is a polynomial function of a order, l:

$$V_h|_{\Omega^{\mathrm{ADD}}(\boldsymbol{b}_h)} = \left\{ v_h \mid (v_h)_i \in C^0\left(\overline{\Omega^{\mathrm{ADD}}(\boldsymbol{b}_h)}\right), (v_h)_i|_{\Omega_j} \in P_l(\Omega_j),\ (v_h)_i = 0 \text{ on } \Gamma_u,\ \forall i(=1,2),\ j(=1,2,\ldots,N_{\mathrm{ae}}) \right\}, \tag{15}$$

$$V_h|_{\Omega} = \left\{ \boldsymbol{v}_h \mid (v_h)_i \in C^0(\overline{\Omega}),\ (v_h)_i|_{\Omega_j} \in P_l(\Omega_j),\ (v_h)_i = 0 \text{ on } \Gamma_u,\ \forall i(=1,2),\ j(=1,2,\ldots,N_e) \right\}. \tag{16}$$

A function, $\boldsymbol{v}_h$ $(\in V_h|_{\Omega^{\mathrm{ADD}}(\boldsymbol{b}_h)})$ can be extended to a unique function, v_h^{ext} $(\in V_h|_{\Omega})$ through being defined as having zero-nodal values on the inactive design domain, Ω^{IADD} $(=\Omega - \Omega^{\mathrm{ADD}})$. The extended function, v_h^{ext} may have nonzero value on the domain of the neighboring elements, $\Omega^{\mathrm{NED}}(\boldsymbol{b}_h)$ of the active design domain, $\Omega^{\mathrm{ADD}}(\boldsymbol{b}_h)$.

In Eq. (13), the following equation is the variational equation for equilibrium for the structure corresponding to a design, $\boldsymbol{b}_h$:

$$a_{\boldsymbol{b}_h}(\boldsymbol{u}_h, \boldsymbol{v}_h) = l_{\boldsymbol{b}_h}(\boldsymbol{v}_h), \quad \forall \boldsymbol{v}_h \in V_h|_{\Omega^{\mathrm{ADD}}(\boldsymbol{b}_h)}. \tag{17}$$

The internal energy, $a_{\boldsymbol{b}_h}(\boldsymbol{u}_h, \boldsymbol{v}_h)$ for a design, $\boldsymbol{b}_h$ is defined on $V_h|_{\Omega^{\mathrm{ADD}}(\boldsymbol{b}_h)} \times V_h|_{\Omega^{\mathrm{ADD}}(\boldsymbol{b}_h)}$ as in Eq. (18). Since the relative density, ρ is bounded from above, the bicontinuity condition, which is defined as in Eq. (19), is satisfied. In Eq. (19), $\|\cdot\|_{m,p,\Omega}$ denote usual norm in the Sobolev space, $W^{m,p}(\Omega)$ (Adams, 1975). Since the relative density, ρ is bounded from below, the uniform ellipticity condition as shown in Eq. (20) is satisfied:

$$a_{\boldsymbol{b}_h}(\boldsymbol{u}_h, \boldsymbol{v}_h) = \int_{\Omega^{\mathrm{ADD}}(\boldsymbol{b}_h)} \rho(\boldsymbol{b}_h) \frac{\partial (\boldsymbol{u}_h)_i}{\partial x_j} \boldsymbol{E}_{ijkl} \frac{\partial (\boldsymbol{v}_h)_k}{\partial x_l} \mathrm{d}\Omega, \tag{18}$$

$$\left| a_{\boldsymbol{b}_h}(\boldsymbol{u}_h, \boldsymbol{v}_h) \right| \leqslant M \|\boldsymbol{u}_h\|_{1,2,\Omega^{\mathrm{ADD}}} \|\boldsymbol{v}_h\|_{1,2,\Omega^{\mathrm{ADD}}}, \quad \forall \boldsymbol{u}_h, \boldsymbol{v}_h \in V_h|_{\Omega^{\mathrm{ADD}}(\boldsymbol{b}_h)},\ \forall \boldsymbol{b}_h \in H_h, \tag{19}$$

$$a_{\boldsymbol{b}_h}(\boldsymbol{u}_h, \boldsymbol{u}_h) \geqslant \alpha \|\boldsymbol{u}_h\|^2_{1,2,\Omega^{\mathrm{ADD}}}, \quad \forall \boldsymbol{u}_h \in V_h|_{\Omega^{\mathrm{ADD}}},\ \forall \boldsymbol{b}_h \in H_h. \tag{20}$$

When defining the set, H_h, several singular designs as shown in Fig. 9, which may not satisfy the ellipticity condition, are excluded. Actually, designs in Fig. 9 are not optimal.

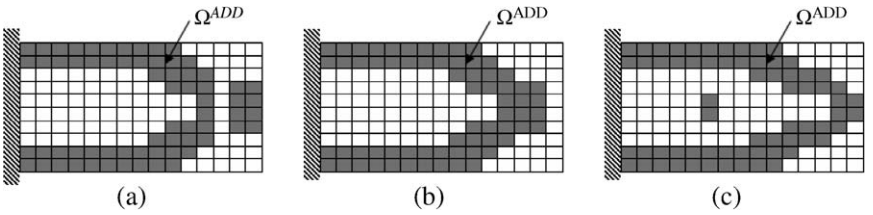

Fig. 9. Excluded designs: (a) Case 1, (b) Case 2 and (c) Case 3.

The external work done by an applied force, $l_{\boldsymbol{b}_h}(\cdot)$ is assumed to satisfy the bounded feature as

$$\|l_{\boldsymbol{b}_h}\| = \sup_{\mathbf{0}\neq \boldsymbol{v}_h \in V_h|_{\Omega^{\mathrm{ADD}}(\boldsymbol{b}_h)}} \frac{|l_{\boldsymbol{b}_h}(\boldsymbol{v}_h)|}{\|\boldsymbol{v}_h\|_{1,2,\Omega^{\mathrm{ADD}}(\boldsymbol{b}_h)}} < +\infty. \tag{21}$$

Given any $h>0$, a pair $(\boldsymbol{u}_h, \boldsymbol{b}_h) \in V_h|_{\Omega^{\mathrm{ADD}}(\boldsymbol{b}_h)} \times H_h$ satisfying the equilibrium condition in Eq. (17) is called an admissible pair in $(\mathrm{MC})_h$. In Eq. (17), there exists an unique displacement solution, $\boldsymbol{u}_h$ $(\in V_h|_{\Omega^{\mathrm{ADD}}(\boldsymbol{b}_h)})$ corresponding to a design, $\boldsymbol{b}_h$, because the bicontinuity condition, Eq. (19) and the uniform ellipticity condition, Eq. (20) holds (Ciarlet, 1978).

Considering Eqs. (17), (20) and (21) for this case, the following bounded feature of $\boldsymbol{v}_h$ $(\in V_h|_{\Omega^{\mathrm{ADD}}(\boldsymbol{b}_h)})$ can be obtained as

$$\|\boldsymbol{v}_h\|_{1,2,\Omega^{\mathrm{ADD}}(\boldsymbol{b}_h)} \leqslant \|l_{\boldsymbol{b}_h}\|/\alpha. \tag{22}$$

For an special case that the active design domain, Ω^{ADD} equals to the whole design domain, Ω, all previous results also hold. Since Eq. (22) holds, the set, $V_h|_\Omega$ defined on the whole design domain, Ω, is weakly sequentially compact (Oden and Demkowicz, 1996).

Let consider a sequence, $\left((\boldsymbol{u}_h)_n^{\mathrm{ext}}, (\boldsymbol{b}_h)_n\right) \in V_h|_\Omega \times H_h$ extended from a sequence of arbitrary admissible pairs, $\left((\boldsymbol{u}_h)_n, (\boldsymbol{b}_h)_n\right) \in V_h|_{\Omega^{\mathrm{ADD}}((\boldsymbol{b}_h)_n)} \times H_h$. Since the set, H_h is compact and the set, $V_h|_\Omega$ is weakly sequentially compact, there is a subsequence, $\left((\boldsymbol{u}_h)_{n_k}^{\mathrm{ext}}, (\boldsymbol{b}_h)_{n_k}\right) \in V_h|_\Omega \times H_h$ of any given sequence, $\left((\boldsymbol{u}_h)_n^{\mathrm{ext}}, (\boldsymbol{b}_h)_n\right) \in V_h|_\Omega \times H_h$ that satisfy

$$\begin{aligned} &(\boldsymbol{u}_h)_{n_k}^{\mathrm{ext}} \to (\boldsymbol{u}_h)^{\mathrm{ext}} \text{ weakly in } V_h|_\Omega, \\ &(\boldsymbol{b}_h)_{n_k} \to \boldsymbol{b}_h \in H_h \text{ uniformly in } R^N \times R^N. \end{aligned} \tag{23}$$

In particular, a minimizing sequence, $\left((\boldsymbol{u}_h)_n, (\boldsymbol{b}_h)_n\right) \in V_h|_{\Omega^{\mathrm{ADD}}((\boldsymbol{b}_h)_n)} \times H_h$ to $(\mathrm{MC})_h$ satisfy

$$\begin{aligned} &(\boldsymbol{u}_h)_{n_k}^{\mathrm{ext}} \to \left(\boldsymbol{u}_h^*\right)^{\mathrm{ext}} \text{ weakly in } V_h|_\Omega, \\ &(\boldsymbol{b}_h)_{n_k} \to \boldsymbol{b}_h^* \in H_h \text{ uniformly in } R^N \times R^N, \end{aligned} \tag{24}$$

for some elements $(\boldsymbol{u}_h^*)^{\mathrm{ext}}$ and $\boldsymbol{b}_h^*$ and some subsequence.

Next, we will show that a pair, $(\boldsymbol{u}_h^*, \boldsymbol{b}_h^*) \in V_h|_{\Omega^{\mathrm{ADD}}(\boldsymbol{b}_h^*)} \times H_h$, which is extracted from an arbitrary pair of cluster points, $\left((\boldsymbol{u}_h^*)^{\mathrm{ext}}, \boldsymbol{b}_h^*\right)$, is coupled through equilibrium (Eq. (17)). Here, $\boldsymbol{u}_h^*$ $(\in V_h|_{\Omega^{\mathrm{ADD}}(\boldsymbol{b}_h^*)})$ is an uniquely determined function from $(\boldsymbol{u}_h^*)^{\mathrm{ext}}$ $(\in V_h|_\Omega)$, which has a same value with $(\boldsymbol{u}_h^*)^{\mathrm{ext}}$ on a domain, $\Omega^{\mathrm{ADD}}(\boldsymbol{b}_h^*)$.

As $(\boldsymbol{b}_h)_{n_k}$ converges uniformly to $\boldsymbol{b}_h^*$ and a function, $F:(\boldsymbol{b}_h)_{n_k}$ $(\in H_h) \to \Omega^{\mathrm{ADD}}$ $(\subset \Omega)$ is continuous, $\Omega^{\mathrm{ADD}}((\boldsymbol{b}_h)_{n_k})$ and $V_h|_{\Omega^{\mathrm{ADD}}((\boldsymbol{b}_h)_{n_k})}$ also converge to $\Omega^{\mathrm{ADD}}(\boldsymbol{b}_h^*)$ and $V_h|_{\Omega^{\mathrm{ADD}}(\boldsymbol{b}_h^*)}$, respectively.

Hence, passing to the limit in Eq. (25), which is an equilibrium equation for a pair of subsequence, $\left((\boldsymbol{u}_h)_{n_k}, (\boldsymbol{b}_h)_{n_k}\right) \in V_h|_{\Omega^{\mathrm{ADD}}((\boldsymbol{b}_h)_{n_k})} \times H_h$, we arrive at Eq. (17):

$$a_{(\boldsymbol{b}_h)_{n_k}}((\boldsymbol{u}_h)_{n_k}, v_h) = l_{(\boldsymbol{b}_h)_{n_k}}(\boldsymbol{v}_h), \quad \forall \boldsymbol{v}_h \in V_h|_{\Omega^{\mathrm{ADD}}((\boldsymbol{b}_h)_{n_k})}. \tag{25}$$

Utilizing the fact that the limit pair is coupled through equilibrium, we can show that the displacement subsequence, $(\boldsymbol{u}_h)_{n_k}^{\text{ext}}$ converges strongly to $(\boldsymbol{u}_h^*)^{\text{ext}}$ in a domain, Ω:

$$\left\|(\boldsymbol{u}_h)_{n_k}^{\text{ext}} - (\boldsymbol{u}_h^*)^{\text{ext}}\right\|_{1,2,\Omega} = \left\|(\boldsymbol{u}_h)_{n_k}^{\text{ext}} - (\boldsymbol{u}_h^*)^{\text{ext}}\right\|_{1,2,\left(\Omega^1((\boldsymbol{b}_h)_{n_k}) \cup \Omega^1(\boldsymbol{b}_h^*)\right)} \tag{26}$$

$$\begin{aligned}
\alpha\left\|(\boldsymbol{u}_h)_{n_k}^{\text{ext}} - (\boldsymbol{u}_h^*)^{\text{ext}}\right\|_{1,2,\Omega^2} &\leqslant a_{(\boldsymbol{b}_h)_{n_k}}\left((\boldsymbol{u}_h)_{n_k} - (\boldsymbol{u}_h^*)^{\text{ext}}|_{\Omega^2}, (\boldsymbol{u}_h)_{n_k} - (\boldsymbol{u}_h^*)^{\text{ext}}|_{\Omega^2}\right) \\
&= a_{(\boldsymbol{b}_h)_{n_k}}\left((\boldsymbol{u}_h)_{n_k} - (\boldsymbol{u}_h^*)^{\text{ext}}|_{\Omega^2}, -(\boldsymbol{u}_h^*)^{\text{ext}}|_{\Omega^2}\right) + a_{(\boldsymbol{b}_h)_{n_k}}\left((\boldsymbol{u}_h)_{n_k}, (\boldsymbol{u}_h)_{n_k}\right) \\
&\quad - a_{(\boldsymbol{b}_h)_{n_k}}\left((\boldsymbol{u}_h^*)^{\text{ext}}|_{\Omega^2}, (\boldsymbol{u}_h)_{n_k}\right) \\
&= a_{(\boldsymbol{b}_h)_{n_k}}\left((\boldsymbol{u}_h)_{n_k} - (\boldsymbol{u}_h^*)^{\text{ext}}|_{\Omega^2}, -(\boldsymbol{u}_h^*)^{\text{ext}}|_{\Omega^2}\right) + l_{(\boldsymbol{b}_h)_{n_k}}\left((\boldsymbol{u}_h)_{n_k}\right) \\
&\quad - a_{(\boldsymbol{b}_h)_{n_k}}\left((\boldsymbol{u}_h^*)^{\text{ext}}|_{\Omega^2}, (\boldsymbol{u}_h)_{n_k}\right)
\end{aligned} \tag{27}$$

In Eq. (26), Ω^1 means the union of Ω^{ADD} and Ω^{NED}. If $\Omega^{\text{ADD}}((\boldsymbol{b}_h)_{n_k})$ converges to $\Omega^{\text{ADD}}(\boldsymbol{b}_h^*)$, $\Omega^1((\boldsymbol{b}_h)_{n_k})$ also converges to $\Omega^1(\boldsymbol{b}_h^*)$. And if the quantity, $\|\cdot\|_{1,2,\Omega^{\text{ADD}}}$ converges to zero, the quantity, $\|\cdot\|_{1,2,(\Omega^{\text{ADD}} \cup \Omega^{\text{NED}})}$ also converges to zero. In Eq. (27), Ω^2 means $\Omega^{\text{ADD}}((\boldsymbol{b}_h)_{n_k})$ and $(\boldsymbol{u}_h^*)^{\text{ext}}|_{\Omega^2}$ is a restriction of $(\boldsymbol{u}_h^*)^{\text{ext}}$ to Ω^2. The first term in Eq. (27) converges to zero and the second term to $l_{\boldsymbol{b}_h^*}(\boldsymbol{u}_h^*)$. The third one converges to $a_{\boldsymbol{b}_h^*}(\boldsymbol{u}_h^*, \boldsymbol{u}_h^*)$, which equals to $l_{\boldsymbol{b}_h^*}(\boldsymbol{u}_h^*)$ by the equilibrium condition.

And passing to the limit in Eqs. (26) and (27), finally we can conclude

$$\begin{aligned}
&(\boldsymbol{u}_h)_{n_k}^{\text{ext}} \to (\boldsymbol{u}_h^*)^{\text{ext}} \text{ strongly in } V_h|_{\Omega}, \\
&(\boldsymbol{b}_h)_{n_k} \to \boldsymbol{b}_h^* \in H_h \text{ uniformly in } R^N \times R^N \quad \text{and} \\
&a_{\boldsymbol{b}_h^*}(\boldsymbol{u}_h^*, \boldsymbol{v}_h) = l_{\boldsymbol{b}_h^*}(\boldsymbol{v}_h), \ \ \forall \boldsymbol{v}_h \in V_h|_{\Omega^{\text{ADD}}(\boldsymbol{b}_h^*)}, \quad l_{\boldsymbol{b}_h^*}(\boldsymbol{u}_h^*) \leqslant l_{(\boldsymbol{b}_h)_{n_k}}\left((\boldsymbol{u}_h)_{n_k}\right).
\end{aligned} \tag{28}$$

4. Numerical examples

In this section, we present the results of two 3D design examples, in order to verify the applicability of MCM for more general problems. To extend the concept and code of MCM to 3D problems, the volume of each material cloud should be treated instead of the area in 2D problems. Objective function is the compliance of a structure with linear elastic behavior. All examples are solved with 20-node quadrilateral finite elements. Except what are noted, all parameters used in the optimization algorithm for MCM and DDM are same.

We recommend you to read Chang and Youn (in press) in advance. You can see various interesting features of MCM, compared with the traditional density approach, because they have treated various examples including typical problems in topology optimization like 2D Michell truss design.

4.1. Example 1: 3D simple support design

The results of MCMPS and DDM are compared for 3D simple example. The problem is defined in Fig. 10. Actually, one quarter model is treated, imposing the symmetry condition. A $40 \times 10 \times 10$ mesh is used. The displacement is constrained to vanish on the left surface of the domain. The volume constraint is $V_0 = 0.1 V_{\text{des}}$. Young's modulus, $E = 70$ GPa and Poisson's ratio, $v = 0.3$.

We compare the results of following three cases. In Case 1, we apply the traditional density-approach (DDM). In Cases 2 and 3, we apply MCMPS. While the initial design domain in Case 2 is the whole design domain, this one in Case 3 is only inner part of the whole design domain, shaded region in Fig. 10(b).

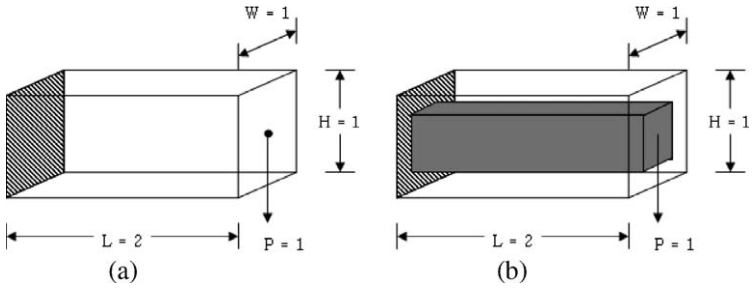

Fig. 10. Problem definition (Example 1): (a) design domain and (b) initial design domain for Case 3.

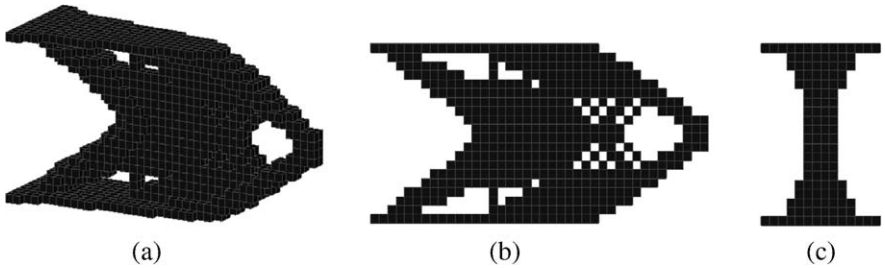

Fig. 11. Optimal material distribution (Example 1, Case 1): (a) 3D view, (b) front view, and (c) side view.

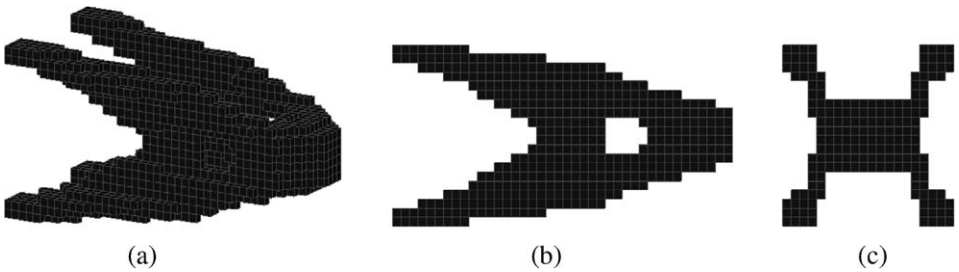

Fig. 12. Optimal material distribution (Example 1, Case 2): (a) 3D view, (b) front view, and (c) side view.

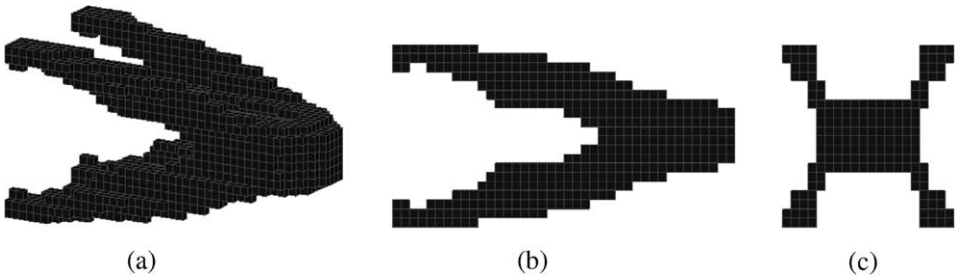

Fig. 13. Optimal material distribution (Example 1, Case 3): (a) 3D view, (b) front view, and (c) side view.

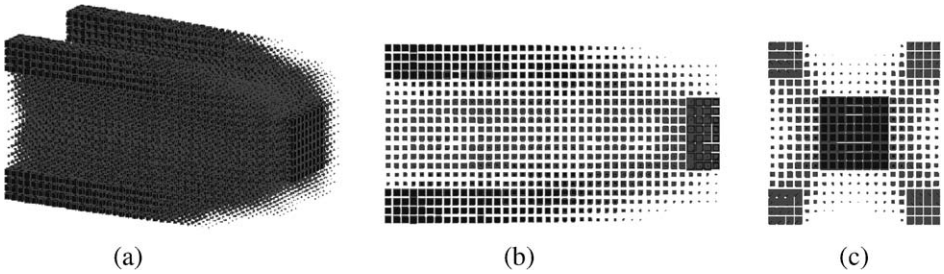

Fig. 14. Initial distribution of material clouds for the subsequent MCMS (Example 1, Case 2): (a) 3D view, (b) front view, and (c) side view.

Figs. 11–13 show the optimal results of Cases 1, 2, and 3, respectively. The optimal material distributions for two cases of MCMPS are quite different from that of DDM. Actually, it can be said that two approaches search different local solutions. From Fig. 14, one can observe the intermediate result of MCM, just after MCMP.

Table 1 compares the results and computational times for three cases. In Table 1, the computational time ratio means the ratio of the computational time of each case to that of DDM (Case 1). Although the optimal results of MCM are somewhat worse than that of DDM, the computational times are significantly saved due to the reduced number of active elements during optimization procedure.

4.2. Example 2: 3D arch-type bridge design

The results of MCMPS and DDM are compared for 3D bridge design problem under a distributed load. The problem is defined in Fig. 15. The optimization problem is modeled as in Fig. 15(b), considering the periodicity of the structure. The upper part of the model is assigned as nondesign domain. Actually, one quarter model is treated, imposing the symmetry condition. A $20 \times 10 \times 22$ mesh is used. The displacement is constrained to vanish on the part of the bottom surface. The volume constraint is $V_0 = 0.2V_{\text{des}}$. The material is a typical concrete. Young's modulus, $E = 30$ MPa and Poisson's ratio, $v = 0.33$.

Table 1
Comparison of the results (Example 1)

	Case 1	Case 2	Case 3
Objective function ($\times 10^{-9}$ N m)	1.3728	1.5914	1.6837
Computational time ratio	1.00	0.74	0.29

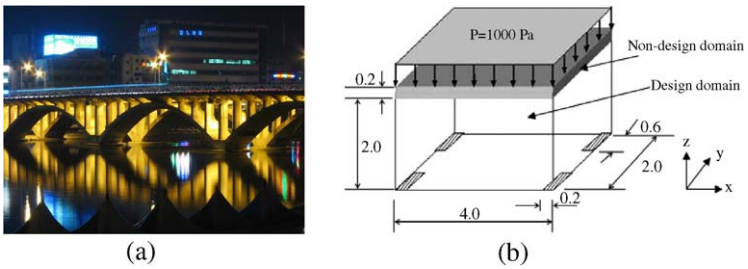

Fig. 15. Problem definition (Example 2): (a) arch-type real bridge and (b) modeling.

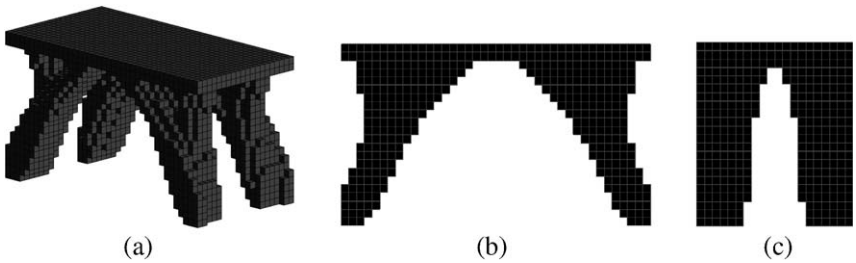

Fig. 16. Optimal design (Example 2, DDM): (a) 3D view, (b) front view, and (c) side view.

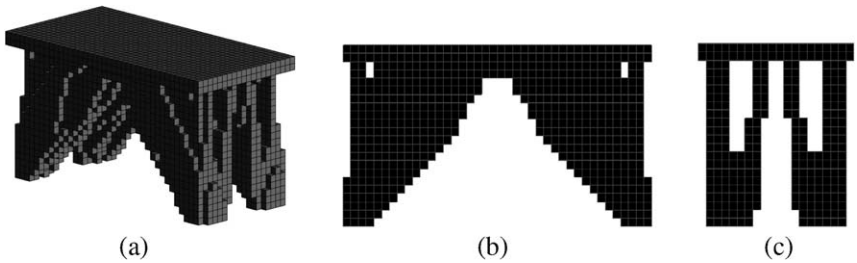

Fig. 17. Optimal design (Example 2, MCMPS): (a) 3D view, (b) front view, and (c) side view.

Figs. 16 and 17 show the optimal results of DDM and MCMPS, respectively. The optimal design for MCMPS is quite different from that of DDM. Main difference is that the optimal result of MCMPS has a hole on the side view and larger support of the top plate. Fig. 18 shows the history of the number of active elements during optimization procedure. In MCMPS, the number of active elements is changed, which is strictly less than the fixed number of DDM, so the computational cost can be significantly reduced.

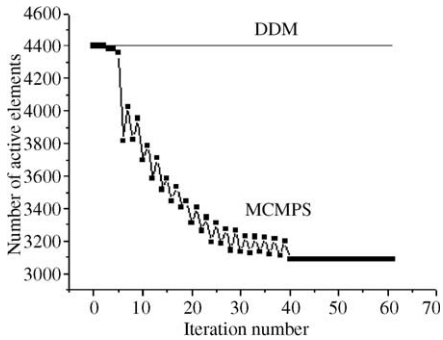

Fig. 18. The history of the number of active elements (Example 2).

Table 2
Comparison of the results (Example 2)

	DDM	MCMPS
Objective function (N m)	1.7151	1.4151
Computational time ratio	1	0.6071

Table 2 compares the results and computational times for DDM and MCMPS. In the case of MCMPS, the better optimal result was obtained with the reduced computational time. However, the result of MCMPS is not always better than that of DDM, since two approaches search different local solutions.

From this numerical experiment, it can be observed that both approaches can produce reasonable optimal results for 3D real bridge design.

5. Conclusions

In this paper, the existence of optimal solution(s) of material cloud method (MCM) is proved for a case of a finite number of material clouds. Therefore, it can be affirmed that the numerical formulation of this method for optimal design is mathematically rigorous. In the mathematical analysis of MCMP, where the active design domain is varied, the one-to-one relationship between displacement functions defined on the admissible design domain and the whole design domain is utilized. Except this idea, all other proving procedure is very similar to that in the case of the density-based approach. It is shown that the cluster-point(s) of a minimizing sequence are included in the design set utilizing the compactness of sets.

However, what is shown in this paper is the existence of solution(s) only for a specific computational mesh. We believe that some additional constraints need to be considered in the problem formulation to ensure the convergence of optimal solutions for different mesh sizes. A research about how to ensure the convergence of optimal solutions in MCM will be a future task.

The application of this method is extended to 3D engineering design problems. To do this, the volume of each material cloud needs to be treated instead of the area in 2D problems. Through several design examples, the generality of MCM can be shown. Coinciding with the anticipated merit of MCM, the computational cost can be significantly saved due to the reduced number of active elements in design domain. But it is observed that the optimal solution may be better or worse than that of the traditional density-based approach depending on the problem, because two methods search different local optimal solutions.

Acknowledgements

The authors thank Martin P. Bendsoe, Department of Mathematics, Technical University of Denmark, for his encouragement and valuable comments on the present work.

This work was supported by the KOrea Science and Engineering Foundation (KOSEF).

References

Adams, R.A., 1975. Sobolev Spaces. Academic Press, New York.

Ambrosio, L., Buttazzo, G., 1993. An optimal design problem with perimeter penalization. Calculus of Variations and Partial Differential Equations 1, 55–69.

Beckers, M., 1999. Topology optimization using a dual method with discrete variables. Structural Optimization 17 (1), 14–24.

Belytschko, T., Xiao, S.P., Parimi, C., 2003. Topology optimization with implicit functions and regularization. International Journal for Numerical Methods in Engineering 57, 1177–1196.

Bendsoe, M.P., 1984. On obtaining a solution to optimization problems for solid, elastic plates by restriction of the design space. Journal of Structural Mechanics 11 (4), 501–521.

Bendsoe, M.P., 1989. Optimal shape design as a material distribution problem. Structural Optimization 1, 193–202.

Bendsoe, M.P., Kikuchi, N., 1988. Generating optimal topologies in structural design using a homogenization method. Computer Methods in Applied Mechanics and Engineering 71, 197–224.

Bendsoe, M.P., Sigmund, O., 2003. Topology Optimization—Theory, Methods and Applications. Springer-Verlag, New York.

Bourdin, B., 2001. Filters in topology optimization. International Journal for Numerical Methods in Engineering 50, 2143–2158.

Chang, S.Y., Youn, S.K., in press. Material cloud method for topology optimization. International Journal for Numerical Methods in Engineering.

Chang, S.Y., Cho, J.H., Youn, S.K., Kim, C.S., Oh, D.H., 2001. Topology optimization of a HDD actuator arm. Computational Structural Engineering 1 (2), 89–96.

Chang, S.Y., Youn, S.K., Kwon, K.C., 2004. Material cloud method—A new topology optimization method. In: 10th AIAA/ISSMO Multidisciplinary Analysis and Optimization Conference, Albany, NY.

Cheng, K.T., Olhoff, N., 1981. An investigation concerning optimal design of solid elastic plated. International Journal of Solids and Structures 17, 305–323.

Ciarlet, P.G., 1978. The Finite Element Method for Elliptic Problems. North-Holland, Amsterdam.

Diaz, A.R., Kikuchi, N., 1992. Solutions to shape and topology eigenvalue optimization problems using a homogenization method. International Journal for Numerical Methods in Engineering 35, 1487–1502.

Jog, C.S., Haber, R.B., 1996. Stability of finite element models for distributed-parameter optimization and topology design. Computer Methods in Applied Mechanics and Engineering 130, 203–226.

Kim, I.Y., Kwak, B.M., 2002. Design space optimization using a numerical design continuation method. International Journal for Numerical Methods in Engineering 53, 1979–2002.

Kim, H., Querin, O.M., Steven, G.P., Xie, Y.M., 2003. Improving efficiency of evolutionary structural optimization by implementing fixed grid mesh. Structural and Multidisciplinary Optimization 24, 441–448.

Liu, J.S., Parks, G.T., Clarkson, P.J., 2000. Metamorphic development: a new topology optimization method for continuum structures. Structural and Multidisciplinary Optimization 20, 288–300.

Ma, Z.D., Kikuchi, N., Cheng, H.C., Hagiwara, I., 1995. Topology optimization technique for free vibration problems. Journal of Applied Mechanics (ASME Transactions) 62, 200–207.

Oden, J.T., Demkowicz, L.F., 1996. Applied Functional Analysis. CRC Press, Boca Raton, FL.

Park, K.S., Chang, S.Y., Youn, S.K., 2003. Topology optimization of the primary mirror of a multi-spectral camera. Structural and Multidisciplinary Optimization 25, 46–53.

Petersson, J., Sigmund, O., 1998. Slope constrained topology optimization. International Journal for Numerical Methods in Engineering 41, 1417–1434.

Querin, O.M., Xie, Y.M., Steven, G.P., 1998. Evolutionary structural optimization (ESO) using a bi-directional algorithm. Engineering Computations 15, 1031–1048.

Sethian, J.A., Wiegmann, A., 2000. Structural boundary via level set and immersed interface methods. Journal of Computational Physics 163 (2), 489–528.

Sigmund, O., 1997. On the design of compliant mechanisms using topology optimization. Mechanics of Structures and Machines 25 (4), 495–526.

Sigmund, O., 2001. Design of multiphysics actuators using topology optimization—Part I: One-material structures. Computer Methods in Applied Mechanics and Engineering 190, 6577–6604.

Svanberg, K., 1987. The method of moving asymptotes—A new method for structural optimization. International Journal for Numerical Methods in Engineering 24, 359–373.

Svanberg, K., 2002. A class of globally convergent optimization methods based on conservative convex separable approximations. SIAM Journal of Optimization 12 (2), 555–573.

Swan, C.C., Kosaka, I., 1997. Voigt-Reuss topology optimization for structures with linear elastic material behaviours. International Journal for Numerical Methods in Engineering 40, 3033–3057.

Xie, Y.M., Steven, G.P., 1993. A simple evolutionary procedure for structural optimization. Computers and Structures 49, 885–896.

Yang, R.J., Chuang, C.H., 1994. Optimal topology design using linear programming. Computers and Structures 52 (2), 265–276.

Yoon, G.H., Kim, Y.Y., 2005. Element connectivity parameterization for topology optimization of geometrically nonlinear structures. International Journal of Solids and Structures 42, 1983–2009.

Youn, S.K., Park, S.H., 1997. A study on the shape extraction process in the structural topology optimization using homogenized material. Computers and Structures 62 (3), 527–538.